J. Fluid Mech. (1975), *vol.* 71, *part* 1, *pp.* 105–122
Printed in Great Britain

On blast waves in exponential atmospheres

By G. G. BACH, A. L. KUHL AND A. K. OPPENHEIM
University of California, Berkeley

(Received 24 January 1975)

The paper presents a comprehensive analysis of gas motion created by a strong explosion in an atmosphere whose density is an exponential function of altitude. For the near field (i.e. short times after initiation), an exact analytical solution of the equations of motion is obtained by means of a perturbation technique. For the far field (i.e. long times after initiation), a similarity solution associated with a logarithmic front trajectory is derived. The two are shown to be well matched with each other. Finally, a fully-algebraic approximate solution is given that qualitatively reproduces all the salient features of the exact and asymptotic solutions, while quantitatively it is in fair agreement with their results.

1. Introduction

Presented here is a study of gas motion initiated by a strong explosion in an exponential atmosphere, a medium whose density varies exponentially with altitude. The flow field of interest is sufficiently large in comparison with the source that it may be treated as resulting from a point explosion, while, as a consequence of the relatively high energy of the wave, counter-pressure effects can be neglected.

In essence, then, the problem is as follows. A finite quantity of energy is released in an exponential atmosphere, generating a strong blast wave. Initially, the latter behaves like a spherical blast in a uniform medium. Shortly thereafter, the exponential dependence of the ambient density on height causes the descending shock front to decay faster than that propagating in the ascending direction. This produces an asymmetry associated with burgeoning of the ascending part of the wave front. Eventually this leads to a 'blow-out' in the ascending direction (i.e. the front reaches infinity in a finite time). Early treatments of this problem were described in Zel'dovich & Raizer (1967). It was speculated by Kompaneets (1960) that perhaps an opposite phenomenon would occur in the descending part (i.e. a complete 'slow-down'), which would involve an infinite amount of time for the front to propagate over a finite distance. However, by now it has been established that this does not take place, whereas the process of 'blow-out' is considered to be physically realistic.

Immediately upon initiation, the blast wave has a structure corresponding to the classical Taylor–Sedov similarity solution; then the motion becomes non-self-similar. However, at later times, both in the ascending and the descending part of the wave, the flow field near the shock front becomes again self-similar. Such similarity solutions were first obtained by Raizer (1964*b*), and later refined

by Hayes (1968*a*, *b*), who expressed the results in the form of integral curves on an appropriate phase plane for the problem, and extended the scope of the analysis to a more general class of problems, by considering the case where the area of the front surface varies exponentially with radius.

The intermediate, non-similar motion was treated by Andriankin *et al.* (1962), who took into account the fact that the shock surface is not normal to the radius vector, causing a non-zero component of the flow velocity in the azimuthal direction. However, they based their analysis on other simplifying assumptions, the most serious being the idealization that the pressure within the blast wave envelope is, at each instant, uniform throughout the flow field. In order to obtain a more realistic solution, and derive proper scaling laws for the flow field, Laumbach & Probstein (1969) performed a careful analysis of the problem (which will be referred to as LP), based on the conservation integrals of the motion. Their approach was based upon recognition of the fact that most of the mass within the blast wave is concentrated near the front, so that the integrands could be expanded into Taylor series about their values at the front and, for the solution, the series truncated to second order. Their results are consequently quite good as long as such truncation can be done with sufficient accuracy, which for the descending part of the wave is indeed the case, even for large times after initiation. However, for the ascending part, the LP solution is valid only over a relatively short period of time (i.e. until the front travels two or three atmospheric scale heights). At later times, the error involved in the truncation becomes more pronounced, leading eventually to an overestimate of the blow-out time.

This problem was treated by Sachdev (1972), on the basis of the method of Brinkley & Kirkwood (1947), which like the LP technique permits a simple analytic solution to be obtained directly from the conservation integrals of the motion. The actual key to Sachdev's solution is a non-dimensional parameter which expresses, in effect, the flow-work performed by the over-pressure along a particle path from the shock to infinity. The value of this parameter is adjusted in such a way that, at large times, it leads to the correct form for the asymptotic motion of the front, irrespective of whether the atmosphere is uniform or not. The results obtained in this way are in fair agreement with LP, as well as with a numerical solution obtained by Lutzky & Lehto (1968) for a blast wave in a spherically symmetric atmosphere where the density increases exponentially with radius in all directions.

Our study of the near field is based on the use of a perturbation technique similar to that of Sakurai (1953). The solution is expressed in the form of a Taylor series, resembling that obtained by Bach & Lee (1969) for a strong implosion. The results are shown to be quite accurate even up to about 10 scale heights, comparing favourably, for short times after initiation, with those of LP. For the far field, a similarity solution is obtained similar to that of Raizer (1964*b*) and Hayes (1968*a*, *b*). The near-field and far-field solutions match sufficiently well with each other to render the extremely difficult analysis of the intermediate flow regime virtually unnecessary. Finally, presented here is an approximate algebraic solution, whose results are in fair quantitative agreement with those obtained by the more elaborate techniques, while qualitatively it reproduces all the properties of the others.

2. Governing equations

Following the LP method, we assume the motion in the azimuthal direction to be negligible, so that the flow is essentially radial, while (as stated in § 1) the explosion is so strong that counter-pressure effects can be neglected. Under such circumstances, assuming also that the medium behaves as a perfect gas with constant specific heat, our problem can be expressed most conveniently in terms of the non-dimensional, expanded form of the conservation equations for the Eulerian space profiles of a point-symmetrical blast wave (see e.g. Oppenheim *et al.* 1972) as

$$\left(\omega-2\frac{f}{x}\right)h-(f-x)\frac{\partial h}{\partial x}-h\frac{\partial f}{\partial x}=\xi\frac{\partial h}{\partial \xi}, \tag{1}$$

$$\frac{\lambda}{2}f-(f-x)\frac{\partial f}{\partial x}-\frac{1}{h}\frac{\partial g}{\partial x}=\xi\frac{\partial f}{\partial \xi}, \tag{2}$$

$$\left(\lambda+\omega-2\gamma\frac{f}{x}\right)g-(f-x)\frac{\partial g}{\partial x}-\gamma g\frac{\partial f}{\partial x}=\xi\frac{\partial g}{\partial \xi}. \tag{3}$$

In the above, $x\equiv r/R$ (where r is the space co-ordinate, while R is the front radius) and $\xi\equiv R/\Delta$ (where Δ is the characteristic scale height of the atmosphere) are the two independent variables. The dependent variables are $f\equiv u/w$ (where u is the particle velocity while w is the front propagation speed), $h\equiv\rho/\rho_a$ and $g\equiv p/\rho_a w^2$ (where ρ and p are the local density and pressure, while ρ_a is the atmospheric density immediately ahead of the front). In addition,

$$\lambda\equiv-2\frac{d\ln w}{d\ln r_n}=-2\frac{d\ln\dot{\xi}}{d\ln\xi} \tag{4a}$$

and

$$\omega\equiv-\frac{d\ln\rho_a}{d\ln r_n}=-\frac{d\ln\rho_a}{d\ln\xi} \tag{4b}$$

are the decay coefficients of the front velocity and of the atmospheric density, respectively, the dot denoting the derivative with respect to time, while γ is the specific heat ratio.

The density of the exponential atmosphere is distributed as

$$\rho_a=\rho_c\exp(-\xi\cos\theta), \tag{5}$$

where ρ_c is the initial value of the atmospheric density at the centre of explosion, while θ is the angle between the front radius vector emanating from the centre of explosion and the vertical. From (4*b*) and (5), it follows that

$$\omega=\xi\cos\theta, \tag{5a}$$

whence for any fixed direction

$$\xi\frac{\partial}{\partial\xi}=\omega\frac{\partial}{\partial\omega}. \tag{5b}$$

In the case of negligible counter-pressure effects, the boundary conditions at the front are given by the strong-shock relations

$$h(1,\xi)=\frac{\gamma+1}{\gamma-1}, \tag{6a}$$

and $$f(1,\xi) = g(1,\xi) = \frac{2}{\gamma+1}. \tag{6b}$$

Moreover, one has the symmetry condition of zero particle velocity in the centre at all times

$$f(0,\xi) = 0. \tag{6c}$$

To determine the front trajectory, one has to take into account the energy of the wave, which, for the case at hand, can be expressed as

$$E_0 = 2\pi \int_0^\pi \mathcal{J} \rho_a w^2 R^3 \sin\theta \, d\theta, \tag{7}$$

where E_0 is the energy of explosion, a constant specified by the explosive charge, while

$$\mathcal{J} \equiv \int_0^1 \left(\frac{g}{\gamma-1} + \frac{hf^2}{2} \right) x^2 \, dx \tag{7a}$$

is the so-called energy integral. Assuming that the explosion energy is equally distributed in all directions, the integration with respect to θ becomes independent of the rest. Thus, introducing the non-dimensional expressions for the front velocity and radius, and taking (5) into account, (7) becomes

$$\frac{E_0}{4\pi\Delta^5\rho_c} = \mathcal{J}\dot{\xi}^2\xi^3 \exp(-\xi\cos\theta) = \text{constant}. \tag{8}$$

Finally, by virtue of (5b), (8) yields the following expression for the decay parameter of the front velocity:

$$\lambda = -2\frac{d\ln\dot{\xi}}{d\ln\omega} = \frac{\omega}{t}\frac{dt}{d\omega} + 3 - \omega, \tag{9}$$

where t is the time co-ordinate. From the latter the dependence of the front velocity and position on time can be evaluated by quadratures.

3. Near field

3.1. *Governing equations*

For the flow field developed at short times after initiation, the governing equations can be solved by adopting ω as the perturbation parameter and expressing the dependent variables in polynomial form, namely

$$\left.\begin{aligned} f &= f_0 + f_1\omega + f_2\omega^2 + \ldots, \\ g &= g_0 + g_1\omega + g_2\omega^2 + \ldots, \\ h &= h_0 + h_1\omega + h_2\omega^2 + \ldots, \\ \lambda &= \lambda_0 + \lambda_1\omega + \lambda_2\omega^2 + \ldots, \end{aligned}\right\} \tag{10}$$

where f_i, g_i and h_i are only functions of x, while the coefficients λ_i are constant.

Upon substitution of the above in (1)–(3), while taking into account (4b), and

grouping coefficients of like powers of ω, one obtains the following set of ordinary differential equations: zero-order,

$$\left.\begin{aligned}(f_0-x)h_0'+h_0f_0' &= -2h_0f_0/x,\\ (f_0-x)f_0'+g_0'/h_0 &= \tfrac{1}{2}\lambda_0 f_0,\\ (f_0-x)g_0'+\gamma g_0f_0' &= \lambda_0 g_0-2\gamma g_0f_0/x;\end{aligned}\right\} \tag{11}$$

first-order,

$$\left.\begin{aligned}(f_0-x)h_1'+h_0f_1' &= -[h_1(1+f_0')-h_0+f_1h_0'+2(h_0f_1+h_1f_0)/x],\\ (f_0-x)f_1'+g_1'/h_0 &= -[f_1(1+f_0'-\tfrac{1}{2}\lambda_0)-\tfrac{1}{2}\lambda_1f_0-h_1g_0'/h_0^2],\\ (f_0-x)g_1'+\gamma g_0f_1' &= -[g_1(1+\gamma f_0'-\lambda_0)-g_0(1+\lambda_1)\\ &\qquad +f_1g_0'+2\gamma(g_0f_1+g_1f_0)/x];\end{aligned}\right\} \tag{12}$$

second-order,

$$\left.\begin{aligned}(f_0-x)h_2'+h_0f_2' &= -[h_2(2+f_0')+h_1(f_1'-1)+f_2h_0'+f_1h_1'\\ &\qquad +2(h_0f_2+h_1f_1+h_2f_0)/x],\\ (f_0-x)f_2'+g_2'/h_0 &= -[f_2(2+f_0'-\tfrac{1}{2}\lambda_0)+f_1(f_1'-\tfrac{1}{2}\lambda_1)-\tfrac{1}{2}\lambda_2f_0\\ &\qquad -h_1g_1'/h_0^2+\{(h_1/h_0)^2-h_2/h_0\}g_0'/h_0],\\ (f_0-x)g_2'+\gamma g_0f_2' &= -[g_2(2+\gamma f_0'-\lambda_0)+g_1(\gamma f_1-\lambda_1-1)-\lambda_2g_0\\ &\qquad +f_2g_0'+f_1g_1'+2\gamma(g_2f_0+g_1f_1+g_0f_2)/x].\end{aligned}\right\} \tag{13}$$

In the above, primes indicate derivatives with respect to x. The boundary conditions at $x = 1$ are

$$h_0(1) = \frac{\gamma+1}{\gamma-1}, \quad f_0(1) = g_0(1) = \frac{2}{\gamma+1}, \tag{14a}$$

$$h_1(1) = f_1(1) = g_1(1) = h_2(1) = f_2(1) = g_2(1) = 0, \tag{14b}$$

while at $x = 0$

$$f_0(0) = f_1(0) = f_2(0) = 0. \tag{14c}$$

The trajectory of the front can be determined by the integration of (9), provided that $\lambda = \lambda(\omega)$ is known. For this purpose we set

$$\mathscr{J} = \mathscr{J}_0+\mathscr{J}_1\omega+\mathscr{J}_2\omega^2+\ldots, \tag{15}$$

where, by substituting the first three expressions of (10) into (7), one has

$$\left.\begin{aligned}\mathscr{J}_0 &= \int_0^1\left(\frac{g_0}{\gamma-1}+\frac{h_0f_0^2}{2}\right)x^2\,dx,\\ \mathscr{J}_1 &= \int_0^1\left(\frac{g_1}{\gamma-1}+\frac{h_1f_0^2}{2}+h_0f_0f_1\right)x^2\,dx,\\ \mathscr{J}_2 &= \int_0^1\left[\frac{g_2}{\gamma-1}+\frac{h_2f_0+h_0f_1^2}{2}+h_0(h_1f_1+h_0f_2)\right]x^2\,dx.\end{aligned}\right\} \tag{16}$$

On the basis of (15), (9) yields

$$\lambda_0 = 3, \quad \lambda_1 = \frac{\mathscr{J}_1}{\mathscr{J}_0}-1, \quad \lambda_2 = 2\frac{\mathscr{J}_2}{\mathscr{J}_0}-\left(\frac{\mathscr{J}_1}{\mathscr{J}_0}\right)^2, \tag{17}$$

representing the desired expressions for the evaluation of λ as implied by the last of (10).

3.2. *Solution*

The various orders of solutions are determined in the following manner.

First, the zeroth-order equations (11) are solved numerically, using the Runge–Kutta technique with boundary conditions specified by (14), and $\lambda_0 = 3$ according to the first of (17). One obtains thus the well-known Taylor–Sedov similarity solution for a strong blast wave of constant energy content. This yields the value of $\mathscr{J}_0$ by virtue of the first expression of (16). With this as a background, one can proceed to the solution of the first-order equations (12), starting from their boundary conditions at the front (i.e. at $x = 1$). This time, however, there is an unknown parameter λ_1 to be determined. This was found by an iterative procedure, based first on the demand that the solution of (12) satisfy the last condition of (14) (i.e. $f_1(0) = 0$), then on assuring oneself that the solution is correct, by evaluating $\mathscr{J}_1$ from (16) and checking the value of λ_1 by using (17). It was found that, using the secant method, only one or two iterations were required to yield values of $|f_1| < 10^{-8}$ at $x = 0$ that satisfied the check based on (16) and (17) with an accuracy of $|\lambda_1| < 10^{-6}$. The second-order equations (13) were treated in a manner similar, with λ_2 as the iteration parameter.

Having found the various coefficients of the polynomial expansions of the dependent variables, one can now determine their profiles by the use of (10) for any fixed (but not too large) value of ω. It turns out, as it will be demonstrated later, that this yields reasonable results up to $|\omega| \sim 10$, a value approaching the similarity solution for the asymptotic regime of the far field. The shock trajectories for various directions and the shock envelope itself are then determined as follows.

According to the last of (10) and the first of (17), the decay parameter can be written as

$$\lambda = 3 + H(\omega),$$

where

$$H(\omega) = \lambda_1 \omega + \lambda_2 \omega^2 + \ldots.$$

Thus, from the definition of λ given by (9), one obtains

$$\frac{d\xi^*}{\xi^*} = -\left[\tfrac{3}{2} + \tfrac{1}{2}H(\omega)\right]\frac{d\xi}{\xi},$$

whence

$$\xi^* = A\xi^{-\frac{3}{2}} \exp\left[-\int_0^{\omega} \frac{H(\omega)}{2\omega}\, d\omega\right]. \tag{18}$$

To evaluate the constant A, we observe that, as $\xi \to 0$, $\xi^* \to A\xi^{-\frac{3}{2}}$. Consequently, expression (8) for the energy of explosion yields

$$A^2 = \frac{E_0}{4\pi\Delta^5 \rho_c \mathscr{J}_0}. \tag{19}$$

This expression lends itself to use as a proper basis for a non-dimensional time scale

$$T = At = t\left[\frac{E_0}{4\pi\Delta^5 \rho_c \mathscr{J}_0}\right]^{\frac{1}{2}}. \tag{20}$$

γ	1·2	1·4	3
λ_1	−0·919651	−0·908483	−0·864823
λ_2	0·0299325	0·0290219	0·0287658
λ_3	—	0·002970	—
$\mathscr{J}_0$	0·85538	0·423289	0·065912
$\mathscr{J}_1$	0·068731	0·038739	0·0089098
$\mathscr{J}_2$	0·015564	0·007915	0·001550
$\mathscr{J}_3$	—	0·001035	—

TABLE 1. Polynomial coefficients for the decay parameter λ, and the non-dimensional energy integral $\mathscr{J}$

The above time scaling parameter differs from that of LP by the factor $(\mathscr{J}_0)^{-\frac{1}{2}}$. In this connexion it is worth noting that, with good approximation, for $\gamma = 1{\cdot}2$ to 1·4,

$$\mathscr{J}_0 \sim \frac{0{\cdot}17}{\gamma - 1},$$

while, for γ as large as 3,

$$\mathscr{J}_0 \sim \frac{0{\cdot}13}{\gamma - 1}.$$

It is, in fact, the above approximation that provided the basis for the derivation of the scaling factor in LP, and its validity has been confirmed by the results of our computations.

In terms of the non-dimensional time scale, (18) can be written as

$$\dot{\xi} \equiv \frac{d\xi}{dT} = \xi^{-\frac{3}{2}} \exp\left[-\int_0^{\omega} \frac{H(\omega)}{2\omega}\, d\omega\right], \tag{21}$$

whence

$$T = \int_0^{\xi} \xi^{\frac{3}{2}} \exp\left[\int_0^{\omega} \frac{H(\omega)}{2\omega}\, d\omega\right]. \tag{22}$$

Using (4*a*), one can obtain from (22) the shock trajectory for any given polar direction θ. In order to determine the shock envelope, (22) is differentiated with respect to θ at constant T, yielding

$$\frac{d\xi}{d\theta} = \left\{1 - \frac{5T}{\left[2\xi^{\frac{5}{2}} \exp\left(\int_0^{\omega} \frac{H(\omega)}{2\omega}\, d\omega\right)\right]}\right\} \xi \tan\theta. \tag{23}$$

Equation (23) can be integrated using the Runge–Kutta technique, both for the ascending (i.e. for $0 < \theta < 90°$) and the descending (i.e. for $90 < \theta < 180°$) direction, by starting from $\theta = 90°$, where $\omega = 0$, while the boundary condition is

$$\xi(90°) = (\tfrac{5}{2}T)^{\frac{2}{5}}.$$

3.3. *Results*

Coefficients of the polynomial expansions for the decay parameter and the energy integral, evaluated by us for various values of γ, are listed in table 1. It is of interest to note that the values of the coefficients for λ are almost independent of

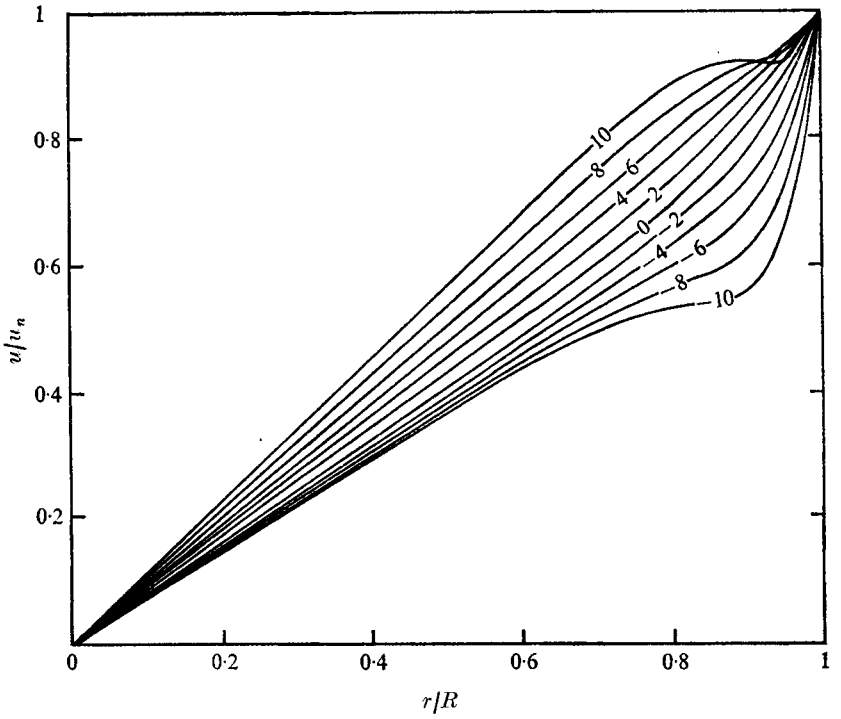

FIGURE 1. Particle velocity profiles for various values of ω, the decay parameter of atmospheric density ($\gamma = 1{\cdot}4$).

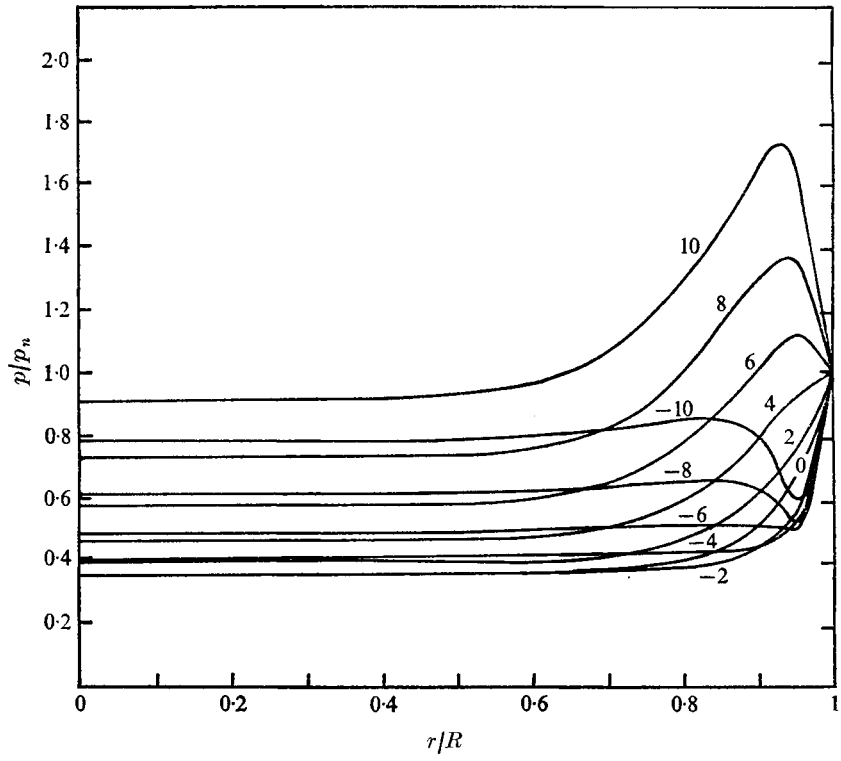

FIGURE 2. Pressure profiles for various values of ω ($\gamma = 1{\cdot}4$).

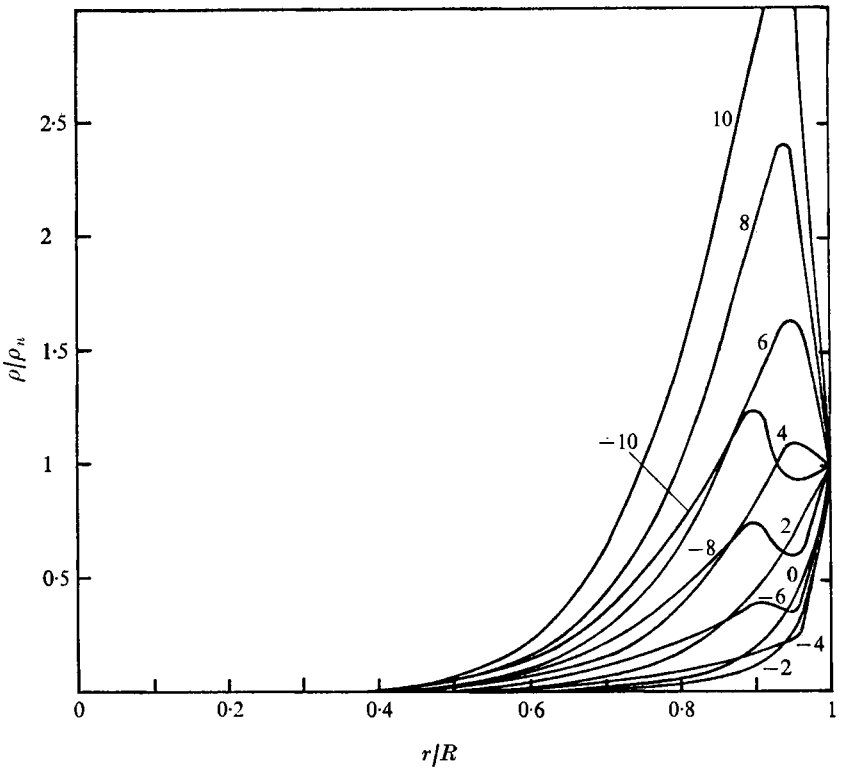

FIGURE 3. Density profiles for various values of ω ($\gamma = 1{\cdot}4$).

γ. In order to obtain an estimate of the validity of the second-order solution, we also evaluated the third-order coefficients for $\gamma = 1{\cdot}4$. According to the power series expansion for λ invoked by (10), it appears from the values of λ_3 and λ_2 that the third-order term will acquire the same order of magnitude as the second-order term when $|\omega| \sim 10$. Hence, it is reasonable to expect that the second-order solution should be quite accurate for $|\omega| < 10$. At the same time, as will be shown later, this is precisely the regime where singular characteristics show a tendency to develop, and the shock motion is then governed primarily by the asymptotic solution valid at later times.

Space profiles of the non-dimensional gasdynamic parameters, the particle velocity f, pressure g, and density h, for $\gamma = 1{\cdot}4$, are given in figures 1–3, respectively, for various values of ω between -10 (in the descending direction) and $+10$ (in the ascending direction). The behaviour of the latter is typically quite similar to that of profiles occurring behind rapidly-accelerating shock fronts, as in the final phases of collapse of an implosion. For the descending direction, the development of a wrinkle in pressure and density profiles close to the front indicates the genesis of a similarity solution.

Figure 4 depicts shock envelopes for various values of T in the case of $\gamma = 1{\cdot}4$. In order to compare our results with the LP solution, we plotted in figure 5 the

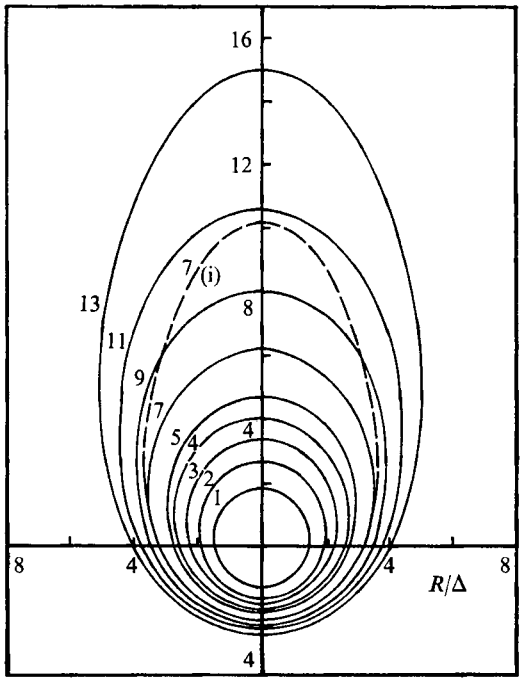

FIGURE 4. Shock envelopes for various values of the non-dimensional time scale $T(\gamma = 1{\cdot}4)$. (i) Approximate analytical solution.

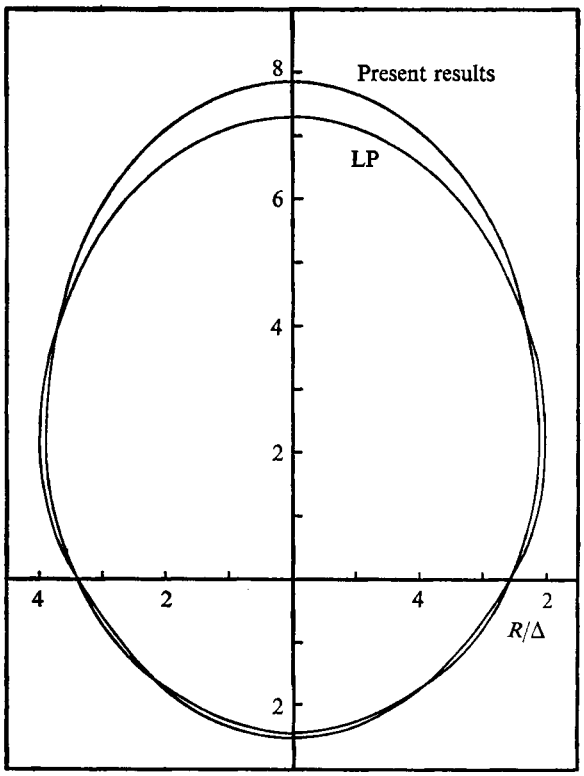

FIGURE 5. Comparison between the shock envelope determined by the present technique and that of LP for $\tau = 8$, corresponding to $T = 8{\cdot}65$ ($\gamma = 1{\cdot}2$).

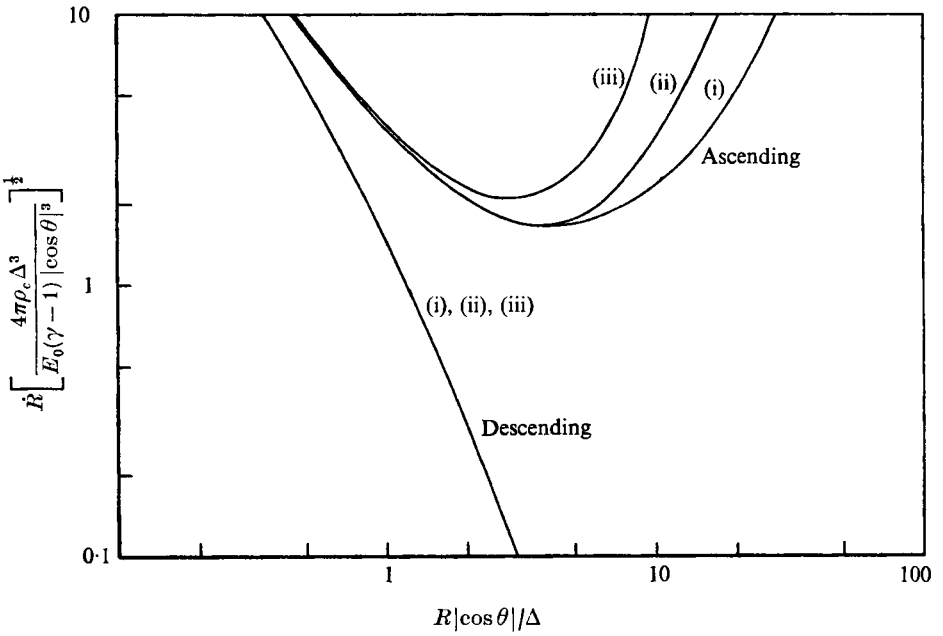

FIGURE 6. Shock velocity as a function of shock position. (i) Results of LP for $\gamma = 1{\cdot}4$. (ii) Present results for $\gamma = 1{\cdot}2$ and $1{\cdot}4$. (iii) Approximate solution.

shock envelope of LP for their $\tau = 8$ and that obtained by us for $T = \tau/\mathscr{J}_0 = 8{\cdot}65$, both in the case of $\gamma = 1{\cdot}2$. As may be seen, the two are practically identical.

The non-dimensional shock velocities as a function of shock radius are presented in figure 6. Our results for $\gamma = 1{\cdot}2$ and $1{\cdot}4$ are shown by curves (i).While these are practically identical to those of LP for $\gamma = 1{\cdot}4$ (curves (ii)) in the descending direction, they differ slightly in the ascending direction, tending toward a shorter blow-out time.

4. Far field

4.1. *Governing equations*

From the preceding results it appears that, as the front radius becomes large, the profiles of flow variables show an ever-increasing tendency to acquire some interesting features immediately behind the front. Moreover, while the values of the variable are bounded, their slopes become quite steep. This is indicative of the approach to the far-field solution corresponding to the limiting case of large $|\xi|$ or, by the same token, large $|\omega|$. In this regime, one can assume that a similarity solution applies, i.e. the terms $\xi\partial/\partial\xi$ on the right-hand side of the governing equations (1)–(3) can be considered negligibly small. In addition, terms involving x^{-1} can also be neglected, since they should be small in the vicinity of the front where $x = 1$, in comparison with those containing the

derivatives with respect to x. Under such circumstances, (1)–(3) become, respectively,

$$\omega h-(f-x)\frac{dh}{dx}-h\frac{df}{dx}=0, \tag{24}$$

$$\tfrac{1}{2}\lambda f-(f-x)\frac{df}{dx}-\frac{1}{h}\frac{dg}{dx}=0, \tag{25}$$

$$(\lambda+\omega)g-(f-x)\frac{dg}{dx}-\gamma g\frac{df}{dx}=0. \tag{26}$$

Also, for a physically meaningful asymptotic solution one must have

$$\lambda=-\beta\omega, \tag{27}$$

where β is a positive constant. The specific reasons for this were given by Hayes (1968*a*, *b*), who represented this property by the formula for the front velocity,

$$\dot{\xi}\cos\theta=\frac{\alpha}{T_B-T}; \tag{28}$$

while his results were expressed in terms of numerical values for the constant α. In (28) T_B represents the blow-out time (i.e. the time at which ξ becomes infinite). A similar relationship is obtained from (27) by taking into account the definitions of λ and ω given by (4), and integrating twice, to derive first an expression for the front velocity, then one for its trajectory. These are, in turn,

$$\dot{\xi}=k\exp(\tfrac{1}{2}\beta\xi\cos\theta), \tag{29}$$

and

$$\exp(-\tfrac{1}{2}\beta\xi_1\cos\theta)-\exp(-\tfrac{1}{2}\beta\xi\cos\theta)=\tfrac{1}{2}k(T-T_1)\beta\cos\theta, \tag{30}$$

where k is a constant of integration, while ξ_1 and T_1 are co-ordinates of an arbitrary reference point of the front trajectory. For $T_1=T_B$, while $\xi_1=\infty$, (29) and (30) yield

$$\dot{\xi}\cos\theta=\frac{2}{\beta(T_B-T)}. \tag{31}$$

It follows from (28) and (31) that

$$\beta=2/\alpha. \tag{32}$$

4.2. *Solution*

As far as the flow field is concerned, the results obtainable from (24)–(26) are valid only within a vanishingly narrow zone behind the front as $|\omega|\to\infty$. Hence, the only interesting problem in this case is the determination of the front trajectory, i.e. the evaluation of the parameter β.

Solution of a self-similar blast-wave problem is, as a rule, reducible to the task of determining an integral curve on an appropriately defined phase plane. Following the technique of Oppenheim *et al.* (1972), the governing equations are reduced for this purpose into a single differential equation, by the introduction of the phase co-ordinates

$$F\equiv f/x \quad\text{and}\quad Z\equiv\gamma g/hx^2. \tag{33}$$

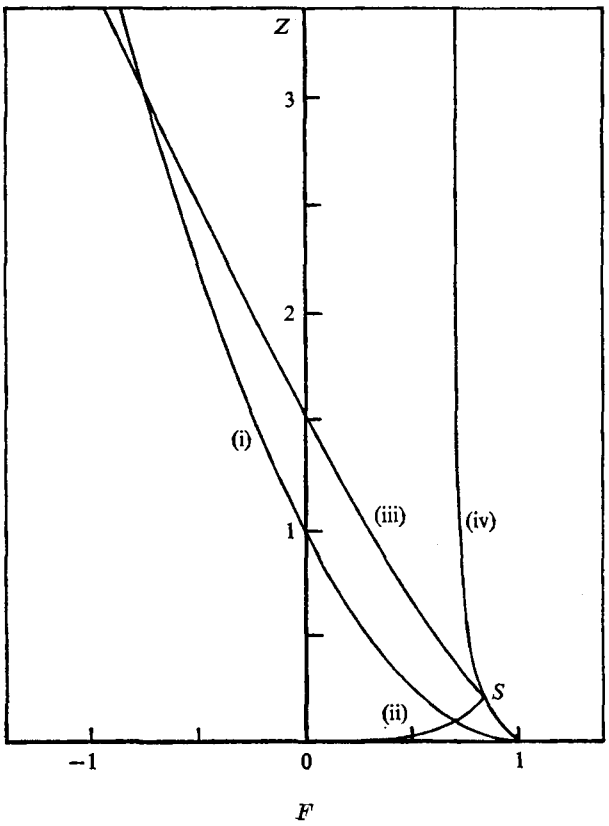

FIGURE 7. Integral curves for $\gamma = 1{\cdot}4$. Point S represents the state immediately behind the shock front. Curve (i) is the locus of saddle points $Z = (1-F)^2$. Curves (ii) and (iii) are similarity solutions for $\beta = 0{\cdot}36810$ (ascending) and $\beta = 1{\cdot}43188$ (descending), respectively. Curve (iv) is the locus of singularities corresponding to the classical Taylor–Sedov solution.

Equations (24)–(26) then yield

$$\frac{dZ}{dF} = \frac{Z}{F-1}\left[\left(\frac{3-\gamma}{2}F-1\right)(F-1)+\frac{1-\beta-\gamma}{\gamma\beta}Z\right]\left[\tfrac{1}{2}F(F-1)+\frac{1-\beta}{\gamma\beta}Z\right]^{-1}, \tag{34}$$

where ω has been eliminated by virtue of (27).

The physically meaningful integral curve satisfying (34) must pass through the point representing the strong-shock boundary conditions, namely

$$F_s = \frac{2}{\gamma+1} \quad \text{and} \quad Z_s = \frac{2\gamma(\gamma-1)}{(\gamma+1)^2}. \tag{35}$$

Moreover, as it is well known, for a physically meaningful solution the integral curve must pass smoothly through the locus of a saddle-point singularity (see figure 7 (i)) specified by the parabola

$$Z = (1-F)^2, \tag{36}$$

γ	1·2	1·4
Ascending	0·30913 (0·309)	0·36810 (0·367)
Descending	1·51704	1·4319 (1·437)

TABLE 2. Critical values for β, the proportionality coefficient between the decay parameters of the front velocity and atmospheric density. (Shown in brackets are the values of $2/\alpha$ obtained by Hayes 1968*a*, *b*.)

i.e. it must coincide with an appropriate axis of the singularity. These conditions are sufficient to determine proper values of β for the ascending as well as the descending part of the blast wave, and, hence, the appropriate integral curves.

Accordingly, then, we proceed as follows. Since the singularity is due only to the second term in (34), we substitute the expression for Z from (36) into the first term, and use the L'Hospital rule for the rest. This yields the quadratic equation for $\chi \equiv dZ/dF$

$$\chi^2 + \frac{(\gamma-1)(\beta-1)F - (\frac{1}{2}\gamma+1) - (\gamma-1)}{1-\beta}\chi - \left[(3-\gamma)F + \frac{1+\gamma}{2}F - \frac{5-\gamma}{2}\right]\frac{\gamma\beta}{1-\beta} = 0. \quad (37)$$

The roots of (37) give the slopes of the two axes of the saddle point for any value of β. There are only two particular values of this parameter for one of the axes at two specific points on the locus of singularities that have physical meaning, and that pass through point S, representing the proper boundary conditions at the front. Its co-ordinates are given by (35). In order to find the proper values of β, we employed a trial-and-error technique, using the Runge–Kutta method to integrate (34), starting from points lying in the close vicinity of the locus of singularities whose co-ordinates were determined by appropriate roots of (37), until $F = F_s$. We considered that the correct value for β was obtained when $|Z - Z_s| < 10^{-8}$.

4.3. *Results*

Critical values of β, evaluated in the manner described above for $\gamma = 1{\cdot}2$ and $1{\cdot}4$, are listed in table 2. Given in brackets are values of $2/\alpha$ based on the results of Hayes (1968*a*, *b*) which, according to (32), should be identical to ours. This is, indeed, practically so; the small deviations are due, no doubt, to different numerical techniques. The corresponding integral curves are presented in figure 7. The lower curve (ii) corresponds to the ascending, the upper (iii) to the descending direction.

It now remains to check how well the near-field solutions match with the asymptotic far-field results. In order to examine the evolution of the flow field, we show in figure 8 integral curves of the near-field solution on the F, Z plane in the neighbourhood of the shock front for various values of ω, together with the asymptotic curve corresponding to $\omega = \infty$ (curve (i)) for the ascending part, and that corresponding to $\omega = -\infty$ (curve (ii)) for the descending part of the blast wave. As may be seen there, slopes of integral curves corresponding to a near-field solution approach that of curve (i) as the positive values of ω increase,

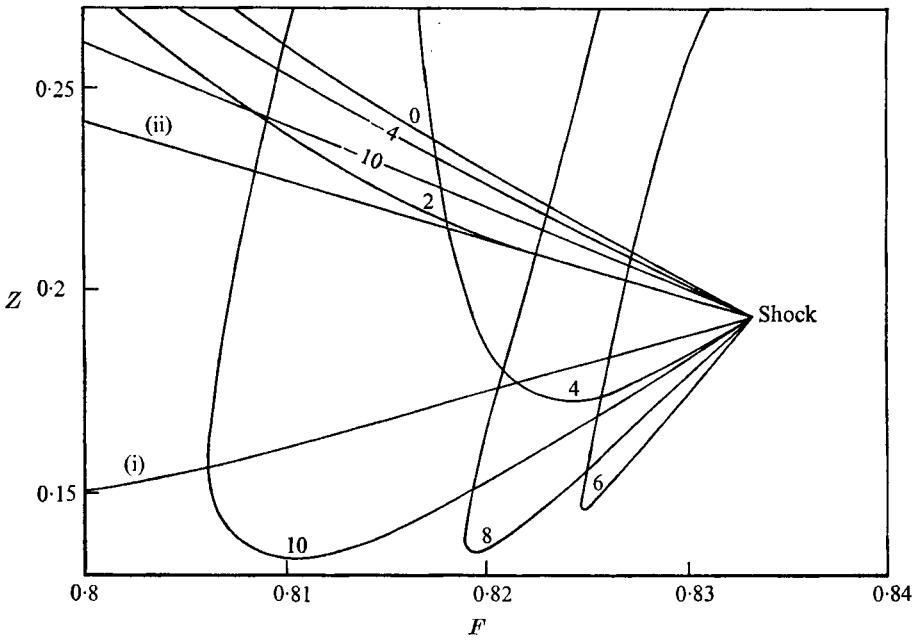

FIGURE 8. Integral curves in the immediate neighbourhood of the shock for various values of $\omega(\gamma = 1{\cdot}4)$. Curves (i) and (ii) are asymptotic similarity solutions for ascending and descending directions respectively.

while integral curves for increasing negative values of ω tend in their entirety towards curve (ii).

With respect to shock trajectories, the most interesting feature is the blow-out time. In order to examine how near-field solutions approach the asymptotes, we employed (31) with $\cos\theta = 1$; ξ was evaluated using (21), and T determined from (22). For direct comparison with LP, the results of this procedure are presented in terms of $\tau = T\mathscr{J}_0^{\frac{1}{2}}$, the time scale of LP. It appears that, for $\omega = 10$, our solution already reaches the asymptotic values of 13·7 for $\gamma = 1{\cdot}2$ and 9·5 for $\gamma = 1{\cdot}4$. However, the corresponding asymptotes of LP are 28·11 and 16·16, respectively, about twice as large as ours. Since our results are in agreement with those of Raizer (1964*a*, *b*) and Hayes (1968*a*, *b*), we are led to the conclusion that the approximation to second order in the integral technique of LP leads to an overestimate of the blow-out time.

5. Approximate solution

Most salient features of blast waves in exponential atmospheres can be described qualitatively by means of a simple approximate solution, based on the notion that the energy integral $\mathscr{J}$ is a relatively insensitive function of ω. This is evident from the coefficient of the polynomial expansion for $\mathscr{J}$ listed in table 1, indicating that this is indeed so, provided that $|\omega|$ is not too large. One can therefore neglect the first term in (9), and assume that

$$\lambda = 3 - \omega. \tag{38}$$

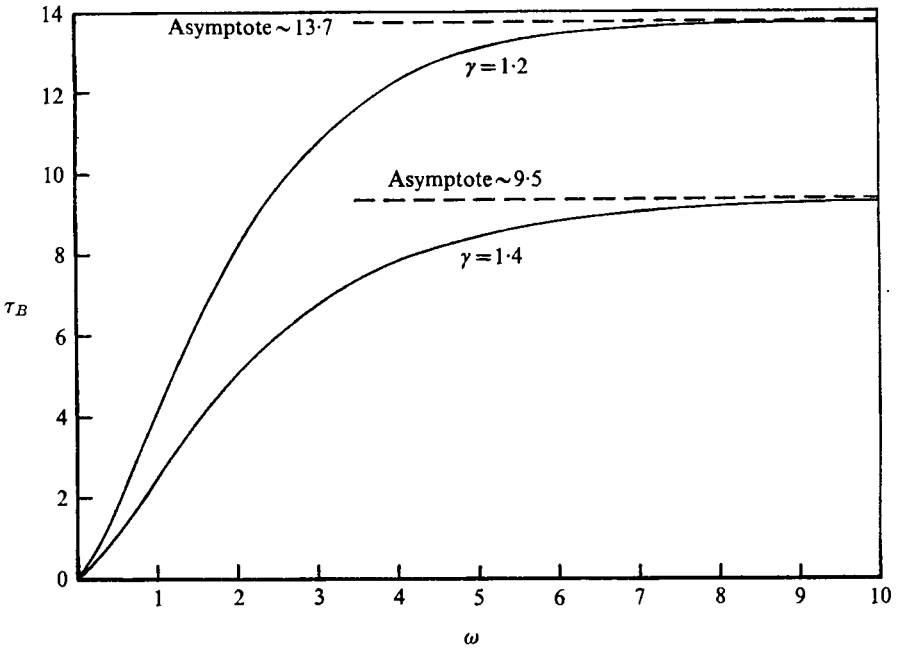

FIGURE 9. Blow-out time τ_B as a function of ω, the decay parameter of atmospheric density.

Equation (38) is the condition for the locus of singularities B, the famous Taylor–Sedov solution, which, as demonstrated by Oppenheim *et al.* (1972), is valid for variable ω. The locus is given by the algebraic equation

$$Z = \frac{\gamma(\gamma-1)}{2} F^2 \frac{1-F}{\gamma F - 1}; \tag{39}$$

and it passes through point S, thus satisfying the strong-shock boundary condition. In figure 7 it is represented by curve (iv). Equation (39) is a particular solution of (34) for $\beta = 1$.

By comparing (38) with the expression for λ used in (18) and (21)–(23), it appears immediately that, for the approximate solution,

$$H(\omega) = \omega.$$

As a consequence of this, (21)–(23) yield straightforward expressions for the front velocities, trajectories, and envelopes, which are independent of γ. In particular, using (4*a*), one obtains for the front trajectory

$$T = \int_0^{\xi} \xi^{\frac{3}{2}} \exp\left(-\tfrac{1}{2}\xi \cos\theta\right) d\xi, \tag{40}$$

which for the blow-out time yields immediately

$$T_B = \int_0^{\infty} \xi^{\frac{3}{2}} \exp\left(-\tfrac{1}{2}\xi\right) d\xi = 2^{\frac{5}{2}}\Gamma(\tfrac{5}{2}). \tag{41}$$

The front envelope of the approximate solution evaluated for $T = 7$ is shown by broken lines in figure 4. The descending part agrees very well with the exact

solution, while the ascending portion grows faster, especially in the vertical direction, acquiring a more oblong shape. The plots of front velocities against position, corresponding to the approximate solution, are given in figure 6 by curves (iii). Here again there is a perfect agreement in the descending direction, while the ascending part exhibits a faster acceleration. In fact, the blow-out time evaluated from (41) is $T_B = 7{\cdot}5468$, in contrast to the more exact asymptotic value of 14·6018.

In spite of the significant discrepancy in the integral curves on the F, Z plane in figure 7, the agreement between front trajectories of the approximate and asymptotic solutions is surprisingly good. Moreover, it is of interest to note that the value of $\beta = 1$ for the approximate solution is practically an average of the two asymptotic values given in table 2.

6. Conclusions

A perturbation solution for the problem of the strong blast waves in an exponential atmosphere has been obtained, which is exact for the near field (i.e. short times following initiation), and is quite accurate even when the front has progressed as much as ten atmospheric scale lengths. This has been matched with an asymptotic far-field solution (i.e. one corresponding to long times after initiation). The latter is independent of the memory of earlier stages, a feature associated with the transition of its integral curve across a saddle point. In addition, a fully-algebraic approximate solution has been found, which is quite accurate for short times after initiation, while exhibiting also many of the important features of the motion at later times.

Characteristic properties of the flow field are expressed in terms of integral curves on an appropriate phase plane for blast waves. Integral curves for the near field and far field are significantly different from that of the classical Taylor–Sedov solution, while the approximate solution represents, in effect, its application to the case of an exponential atmosphere, a property that has not been realized before.

As far as the motion of the front is concerned, the matching between the near-field and far-field solutions has been shown to be so good that the determination of an intermediate solution became unnecessary. The agreement between the results of the exact and approximate solutions for the motion of the front into the denser medium is most satisfactory. For the motion into the rarefying atmosphere, there are some deviations leading to an underestimate, by a factor of almost two, of the blow-out time, i.e. the time at which the velocity of the front becomes infinite.

This work was supported by the United States Air Force, through the Air Force Office of Scientific Research, under grant AFOSR-72-2200, and by the National Science Foundation, under grant NSF Gk-41614.

REFERENCES

ANDRIANKIN, E. I., KOGAN, A. M., KOMPANEETS, A. S. & KRAINOV, V. P. 1962 The propagation of a strong explosion in a non-homogeneous atmosphere. *Zh. Prikl. Mekl. Tekl. Fiz.* **6**, 3.

BACH, G. G. & LEE, J. H. 1969 Initial propagation of impulsively-generated converging cylindrical and spherical shock waves. *J. Fluid Mech.* **37**, 513.

BRINKLEY, S. R. & KIRKWOOD, J. G. 1947 Theory of the propagation of shock waves. *Phys. Rev.* **71**, 606.

HAYES, W. D. 1968*a* Self-similar strong shocks in an exponential medium. *J. Fluid Mech.* **32**, 305.

HAYES, W. D. 1968*b* The propagation upward of a shock wave from a strong explosion in the atmosphere. *J. Fluid Mech.* **32**, 317.

KOMPANEETS, A. S. 1960 A point explosion in an inhomogeneous atmosphere. *Soviet Phys. Doklady*, **5**, 46.

LAUMBACH, D. D. & PROBSTEIN, R. F. 1969 A point explosion in a cold exponential atmosphere. *J. Fluid Mech.* **35**, 53.

LUTZKY, M. & LEHTO, D. L. 1968 Shock propagation in spherically symmetric exponential atmospheres. *Phys. Fluids*, **11**, 1466.

OPPENHEIM, A. K., KUHL, A. L., LUNDSTROM, E. A. & KAMEL, M. M. 1972 A parametric study of self-similar blast waves. *J. Fluid Mech.* **52**, 657.

OPPENHEIM, A. K., LUNDSTROM, E. A., KUHL, A. L. & KAMEL, M. M. 1972 A systematic exposition of the conservation equations for blast waves. *J. Appl. Mech.* p. 783.

RAIZER, YU. P. 1964*a* Motion produced in an inhomogeneous atmosphere by a plane shock of short duration. *Soviet Phys. Doklady*, **8**, 1056.

RAIZER, YU. P. 1964*b* The propagation of a shock wave in a non-homogeneous atmosphere in the direction of decreasing density. *Zh. Prikl. Mekl. Tekl. Fiz.* **4**, 49.

SACHDEV, P. L. 1972 Propagation of a blast wave in uniform or non-uniform media: a uniformly valid analytic solution. *J. Fluid Mech.* **52**, 369.

SAKURAI, A. 1953 On the propagation and structure of blast waves. *J. Phys. Soc. Japan*, **8**, 662.

SEDOV, L. 1957 *Similarity and Dimensional Methods in Mechanics* (4th edn). Academic.

TAYLOR, G. I. 1950 The formation of a blast wave by a very intense explosion. *Proc. Roy. Soc.* A **201**, 159.

ZEL'DOVICH, YA. B. & RAIZER, YU. P. 1967 *Physics of Shock Waves and High Temperature Hydrodynamic Phenomena*, vol. 2. Academic.